

DUANLIE

YU PILAO

JI JIEGOUANQUANXING  
PINGDING

断裂与疲劳  
及结构安全性评定

主 编 康国政 杨翊仁



西南交通大学出版社  
[Http://press.swjtu.edu.cn](http://press.swjtu.edu.cn)

# 断裂与疲劳及结构安全性评定

主编 康国政 杨翊仁

西南交通大学出版社

· 成 都 ·

-----  
**图书在版编目 ( C I P ) 数据**

断裂与疲劳及结构安全性评定 / 康国政, 杨翊仁主  
编. —成都: 西南交通大学出版社, 2009.11  
ISBN 978-7-5643-0474-4

I. ①断… II. ①康…②杨… III. ①断裂力学—文  
集②疲劳断裂—文集③结构安全度—文集 IV.  
①0346.1-53

中国版本图书馆 CIP 数据核字 (2009) 第 191042 号  
-----

**断裂与疲劳及结构安全性评定**

主编 康国政 杨翊仁

\*

责任编辑 李芳芳

封面设计 墨创文化

西南交通大学出版社出版发行

成都二环路北一段 111 号 邮政编码: 610031 发行部电话: 028-87600564

<http://press.swjtu.edu.cn>

四川森林印务有限责任公司印刷

\*

成品尺寸: 185 mm×260 mm 印张: 17 插页: 2

字数: 425 千字

2009 年 11 月第 1 版 2009 年 11 月第 1 次印刷

**ISBN 978-7-5643-0474-4**

定价: 49.80 元

图书如有印装质量问题 本社负责退换  
版权所有 盗版必究 举报电话: 028-87600562

# 序 言

材料和结构的断裂、疲劳及安全性评定是固体力学研究的重要问题。多年来，上述问题的研究已经在多方面取得了重要进展。研究成果既深化了对力学基础理论的认识，又发展了各具特色的试验技术和理论分析方法，解决了工程中的许多重大技术问题。近年来，随着科技、经济的发展，各类新材料不断涌现，材料与结构的服役条件更趋复杂多变，这对断裂、疲劳及结构安全性评定的研究提出了新的挑战；同时各种新技术的出现也为我们发展新的试验测试技术和新的分析计算方法提供了可能。这些都促使疲劳、断裂、损伤以及工程结构安全性评定方面的研究，呈现出学科交叉、领域拓宽、研究深化以及相关成果在诸多领域更广泛应用的新趋势和新局面。

高庆教授长期从事固体破坏及工程结构安全评定等领域的研究和教学工作，是西南交通大学力学学科博士点和博士后流动站的主要学术学科带头人和创建者之一，在固体断裂、疲劳、损伤以及材料本构关系等方面取得了一系列重要成果，是国内该领域的知名专家。同时，她治学严谨、教书育人，倡导创新教育，认真实践从“知识、能力、素质”三方面培养人才，培养了一大批硕士生、博士生和博士后，获得全国百篇优秀博士论文导师奖。高庆教授曾任中国创造学会副理事长，中国力学学会理事及断裂与损伤专业组成员，中国机械工程学会失效分析专业委员会委员，《固体力学学报》编委，四川省力学学会理事长，四川省青年基金会理事长，四川省学位委员会学科评议组专家等职。

在高庆教授 70 寿辰之际，为了彰显高庆教授在科学研究、人才培养方面的突出成就，同时，也为了反映近些年来，在断裂与疲劳、材料本构关系和结构安全性评定领域取得的一些重要研究进展，特出版《断裂与疲劳及结构安全性评定》一书。

本论文集共收集了国内外作者的 36 篇论文。内容不仅包括断裂与疲劳、材料本构关系和结构安全性评定的理论、计算和试验方法及其在工程领域的应用，也反映了力学与物理、生物、材料、微电子等学科交叉研究的最新进展。该论文集不仅涉及复合材料、金刚石膜、钎料合金、树脂、橡胶等新型材料的疲劳、断裂、损伤研究，也涉及高温结构、微电子封装结构、高速列车转向架结构、隧道盾构结构、核反应堆结构和电力结构等复杂工程结构。论文集既注重对基本力学理论的深化认识，又注重各具特色的试验测

试技术、理论分析方法和数值模拟技术的发展和工程应用。

作为本论文集的编者，我们衷心感谢所有作者，是他们精心撰写的高水平学术论文，保证了本论文集的质量。除两位主编外，西南交通大学力学与工程学院的沈火明教授、张娟副教授、李丹柯老师和刘宇杰博士等都参与了本论文集的论文收集、整理和出版工作，在此表示衷心感谢。同时，感谢西南交通大学出版社对本论文集的出版给予的大力支持。限于时间和经验的不足，本论文集存在的不妥之处敬请各位专家和读者批评指正。

衷心祝贺高庆教授 70 寿辰健康快乐！

康国政 杨翊仁

2009 年 10 月

**謹以此文集庆贺高庆教授七十寿辰！**



高庆教授近照

# 目 录

## 论 文

Surface Instability of Soft Polymer Fibers in Electrospinning .....	Bo LI Xiqiao FENG Shouwen YU	3
高温结构完整性原理的构建.....	涂善东	11
结构的概率设计与可靠性指标分析.....	曾攀 李婉宜 雷丽萍	18
超声加速试验方法及超长寿命疲劳问题研究.....	王清远	24
微电子封装可靠性设计中的强度失效.....	陈旭	31
Elastic-Plastic Fracture Mechanics Analysis of Surface Cracked Plates.....	Xin WANG	37
相对性与牛顿三定律的关系.....	黄永畅	48
秦二扩热段温度计套管管座疲劳分析.....	张世伟 陈学德 沈双全	52
含故障参数转向架模型的动力学分析与半主动控制.....	赵娜 曹登庆	57
采用复合法提高拒绝抽样技术效率的探讨.....	刘长虹	67
不同 $KC$ 数下振荡圆柱的流场分析.....	李田 张继业	73
微分求积方法及其在流体力学中的应用.....	李鹏 杨翊仁	79
两种蠕变-疲劳交互作用损伤模型的比较.....	崔瑞乾 戴振羽	87
摩擦对 316L 不锈钢粉末烧结尺寸变化的影响 .....	钟叙 石建军 成志强 柳葆生	91
GCr15/LZ50 扭转微动磨损损伤行为研究.....	刘娟 沈火明 蔡振兵 朱昱昊	95
地铁盾构隧道施工力学分析与数值模拟.....	李新军 喻勇	101
ANSYS 在预应力混凝土连续梁桥内力分析中的应用.....	罗超 丁桂保	106
考虑抛光效应的血管支架有限元分析.....	武亮亮 杨杰 马术文	112
三角翼机翼抖振研究.....	张明禄	118
预紧螺栓连接的塑性变形行为.....	杨显杰 吴志俊	123
橡胶隔振器的动态本构行为研究 .....	林松 张鲲 孙磊 王旭 刘理涛 李天勇	127
A Nonlocal Damage Constitutive Model on Solder Material.....	Jianghui MAO	132
循环软化材料在应变循环与棘轮变形下的塑性模量演化 .....	罗艳 杨显杰 蔡力勋	151
接触力学中不服从 Hertz 接触压力分布的几个方面.....	肖华磊 江晓禹	159
颗粒、纤维增强复合材料界面特性的研究现状.....	马莉 江晓禹	164



基于载荷分离理论的单试样法研究综述	包陈 蔡力勋	169
超临界 W 火焰锅炉炉膛负荷分析	杜长城 冉燊铭 李映辉	180
复合材料风机叶片疲劳损伤计算方法研究	王静 黄志华 李映辉	186
历史概率疲劳 S-N 曲线的 Monte Carlo 模拟与修正	赵永翔 杨冰	194
工程材料的棘轮行为与棘轮-疲劳交互作用研究	康国政	202
材料超高周疲劳性能研究	王弘	208
金刚石膜沉积系统中等离子体的流动与传热研究	唐达培 李映辉	214
描述循环硬化材料非比例多轴循环变形行为的本构模型的有限元实现	张娟 康国政	221
304 不锈钢高温多轴时相关低周疲劳试验研究	刘宇杰 高庆 罗艳	228
六轴机车横向运动稳定性研究	高学军 李映辉 高庆	233
PEEK 树脂单轴应变循环特性及时间相关棘轮行为的试验研究	潘斗兴 朱志武 康国政 刘宇杰	241

## 高庆教授简介

高庆教授简介	康国政 整理	249
高庆教授论著目录		251
高庆教授获奖情况		264

# 论 文

•

# Surface Instability of Soft Polymer Fibers in Electrospinning

Bo LI Xiqiao FENG Shouwen YU

AML, Department of Engineering Mechanics, Tsinghua University, Beijing 100084, China

## 【 Abstract 】

In order to elucidate the observed pattern formation on the surfaces of some electrospun polymer fibers, we investigate the surface wrinkling of soft fibers induced by surface charges via linear stability analysis. The analytical solutions are derived for the critical conditions for the occurrence of surface instability and the wavelength of the induced surface patterns. It is found that the instability characteristic can be modulated by varying the surface charge density. Besides the destabilizing effect of surface charges, surface tension plays a Rayleigh-like destabilizing role in the surface evolution process. In addition, the morphological evolution of a soft fiber is demonstrated to exhibit distinct dependence on its diameter and surface tension.

## 【 Keywords 】

surface instability; polymer fiber; linear stability analysis; electrospinning

## 1 Introduction

Polymer fibers hold great promise for extensive applications in a wide range of engineering fields. Especially, polymer nanofibers have a large surface area to volume ratio and unique nanometer scale architecture and, therefore, are good candidates for applications in medicine, biotechnology, and nanoelectronic devices and systems. Among other, electrospinning has been proved to be an efficient way to produce nanofibers from molten or solution polymers by applying an electric field <sup>[1]</sup>. This non-mechanical, electrostatic technique involves the use of a high voltage electrostatic field to charge the surface of a polymer solution droplet and thus to induce the ejection of liquid jet with diameter in the range of 100 nm through a spinneret <sup>[2]</sup>.

However, experiments evidence that the polymer fibers obtained by electrospinning are prone to lose their surface stability, which consequently leads to the formation of surface morphologies on the fibers. On one hand, the surface instability may cause damage or even rupture of the fibers, placing a limitation to their industrial applications <sup>[1]</sup>. On the other hand, nanofibers with surface patterns of characteristic wavelength may exhibit some unique properties and find some technologically important applications. For example, superhydrophobic properties might be achieved by introducing surface microstructures on the fibers. Although considerable effort has

been directed toward understanding the morphological evolution of planar surfaces [3-8], there is a shortage of investigations on the wrinkling of curved surfaces [9-11]. The present paper aims to elucidate the surface evolution of soft polymer cylinders with surface charges. This issue is of great interest not only for electrospinning techniques but also for such fields as surface science and biophysics [12].

## 2 Model

We study the morphological instability of soft polymer fibers with uniformly distributed surface charges. The material is treated as an incompressible viscous fluid, as in some previous studies [3-6, 9, 11]. Refer to a cylindrical coordinate system  $(r, \theta, z)$ , where its origin is located at the central axial of the originally cylindrical fiber of radius  $R$ , as shown in Fig. 1. Let  $\rho$  denote its surface charge density. The cylinder is assumed to be sufficiently long such that no effect of its ends needs to be considered.

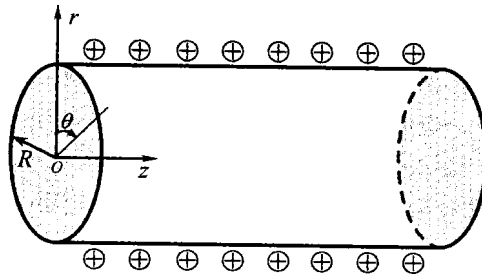


Fig. 1 A soft cylindrical fiber with surface charges

## 3 Instability analysis

We adopt the linear stability analysis method, in which a small perturbation is superposed on the cylinder surface. For a very long cylindrical surface, there exist two possible types of surface instability, leading to axial and circumferential patterns, respectively. They may occur separately or simultaneously on its surface, depending upon the surface charge density, the curvature and surface property of the fiber. The simultaneous occurrence of the two types of instability will lead to a three-dimensional surface pattern, as illustrated in Fig. 2. Introduce a complete sinusoidal perturbation in the form of  $r(\theta, z, t) = R + \delta(t) \cos(n\theta) \cos(\omega z)$ . Here  $n$  and  $\omega$  denote the circumferential mode and axial wavenumber, respectively,  $\delta(t)$  is the perturbation amplitude satisfying  $\delta(t)/R \ll 1$ , and  $t$  denotes time. For the linear stability analysis presented here, all non-linear terms of  $\delta(t)$  can be neglected.

From the continuity and Navier-Stokes equations simplified with the long wave approximation, the surface evolution of the fiber is described by [5]

$$\partial r / \partial t = -\nabla \cdot \mathbf{J} \quad (1)$$

where  $\nabla$  denotes the gradient operator and  $\mathbf{J}$  the pressure-driven flux in the polymer fiber.  $\mathbf{J}$  depends on the pressure  $p$  via the relation

$$\mathbf{J} = -r^3 \nabla p / (3\mu) \quad (2)$$

where  $\mu$  is the viscosity of the soft fiber. The pressure  $p$  in the fiber involves three contributions, namely

$$p = p_0 + p_{\text{Lap}} + p_{\text{el}} \quad (3)$$

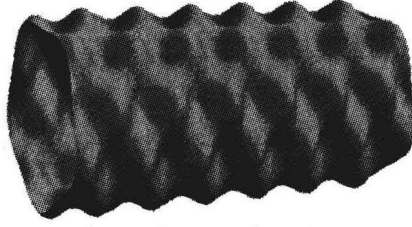


**Fig. 2 Three-dimensional morphology of surface instability**

where  $p_0$  is the environmental pressure,  $p_{\text{el}}$  is the electrostatic pressure originating from the Maxwell stress, and  $p_{\text{Lap}} = \gamma\kappa$  is the Laplace pressure, with  $\gamma$  being the surface energy density per unit area and  $\kappa$  the surface curvature. Due to the presence of the small sinusoidal perturbation, the surface curvature  $\kappa$  and the outward unit vector  $\mathbf{n}$  normal to the surface become

$$\kappa(\theta, z) = \frac{1}{R} + \left( \frac{n^2 - 1}{R^2} + \omega^2 \right) \delta \cos(n\theta) \cos(\omega z) \quad (4)$$

$$\mathbf{n} = \mathbf{e}_r + \delta \frac{n}{R} \sin(n\theta) \cos(\omega z) \mathbf{e}_\theta + \delta \omega \cos(n\theta) \sin(\omega z) \mathbf{e}_z \quad (5)$$

where  $\mathbf{e}_r$ ,  $\mathbf{e}_\theta$ , and  $\mathbf{e}_z$  are the unit vectors in the radial, circumferential, and axial directions, respectively.

The electric field  $\mathbf{E}$  and the electric potential  $\psi$  around the fiber satisfy the equations  $\mathbf{E} = -\nabla\psi$  and  $\Delta\psi = 0$ , where  $\Delta$  denotes the Laplacian operator. The electric field contains two parts, i.e.,

$$\mathbf{E} = \bar{\mathbf{E}} + \tilde{\mathbf{E}} \quad (6)$$

where an overbar and a tilde stand for the quantities in the initial state before perturbation and in the perturbed state, respectively. In the initial state, one has  $\bar{\mathbf{E}} = (E_0 R / r) \mathbf{e}_r$ , where  $E_0 = \rho / \varepsilon$  with  $\varepsilon$  being the permittivity of the air or fluid outside the fiber. The electric potential induced by the perturbation takes the form

$$\tilde{\psi} = [a I_n(\omega r) + b K_n(\omega r)] \cos(n\theta) \cos(\omega z) \quad (7)$$

where  $I_n(\omega r)$  and  $K_n(\omega r)$  are the first and second modified Bessel functions of the  $n$ -th order, respectively,  $a$  and  $b$  are constants to be determined. The boundary conditions require that

$n \times E = 0$  on the fiber surface ( $r = R$ ) and  $E \rightarrow 0$  at infinity. From these two conditions, we obtain  $a = 0$  and  $b = \delta E_0 / K_n(\omega R)$ . Hence, the electric field induced by the surface perturbation can be easily derived via  $\vec{E} = -\nabla \tilde{\psi}$ . Then the electrostatic pressure  $p_{el}$  is calculated to the first order of the perturbation amplitude  $\delta$  as <sup>[13]</sup>

$$p_{el} = -\frac{1}{2} \epsilon E^2 = -\frac{\epsilon E_0^2}{2} \left\{ 1 + \frac{\delta \omega [K_{n-1}(\omega R) + K_{n+1}(\omega R)]}{K_n(\omega R)} \cos(n\theta) \cos(\omega z) \right\} \quad (8)$$

Then from Eq. (3), the total pressure  $p$  in the fiber is determined as

$$p = \left( p_0 + \frac{\gamma}{R} - \frac{\epsilon E_0^2}{2} \right) + \left\{ \gamma \left( \frac{n^2 - 1}{R^2} + \omega^2 \right) - \frac{\epsilon E_0^2 \omega [K_{n-1}(\omega R) + K_{n+1}(\omega R)]}{2 K_n(\omega R)} \right\} \delta \cos(n\theta) \cos(\omega z) \quad (9)$$

Substituting Eq. (9) into (1) and applying (2) and (4) leads to  $d\delta/dt = \tau\delta$ . Integrating this equation, one obtains the temporal evolution equation of surface perturbation:  $\delta(t) = \delta_0 \exp(\tau t)$ , where  $\delta_0$  denotes the perturbation amplitude at  $t = 0$ . The parameter  $\tau$  evaluates the growth of surface evolution and is referred to as the growth rate <sup>[9]</sup>. Its analytical solution is

$$\tau = \frac{R^3}{3\mu} \left( \frac{n^2}{R^2} + \omega^2 \right) \left\{ -\gamma \left( \frac{n^2 - 1}{R^2} + \omega^2 \right) + \frac{\epsilon E_0^2 \omega [K_{n-1}(\omega R) + K_{n+1}(\omega R)]}{2 K_n(\omega R)} \right\} \quad (10)$$

When  $\tau < 0$ , the amplitude of the initial perturbation will decay exponentially with time, indicating that the fiber surface is stable with respect to the perturbation. When  $\tau > 0$ , on the other hand, the fiber surface is unstable and the perturbation amplitude will be exponentially magnified with time. It can be seen from Eq. (10) that the electrostatic pressure always tends to destabilize the cylinder surface since  $K_n(\omega r) > 0$  holds for any nonzero  $\omega$ .

By setting  $\tau = 0$  in Eq. (10), a critical state of surface morphological evolution can be determined and we obtain the critical perturbation of surface instability with a particular mode, characterized by  $(n_c, \omega_c)$ . For a given fiber radius  $R$ , one can obtain the critical charge density  $\rho_c$  above which the fiber surface morphology will become unstable

$$\rho_c = \sqrt{\frac{2\epsilon\gamma K_n(\omega R)[n^2 - 1 + (\omega R)^2]}{\omega R^2 [K_{n-1}(\omega R) + K_{n+1}(\omega R)]}} \quad (11)$$

When the surface charge density  $\rho$  exceeds the threshold  $\rho_c$ , the originally cylindrical fiber will be buckled due to the large electrostatic pressure and an ordered surface pattern will appear on its surface. Among all possible perturbation modes, the characteristic surface pattern corresponding to the fastest growth rate is regarded as the most probable mode to appear, denoted by  $(n_f, \omega_f)$ . It can be determined by

$$\frac{\partial \tau}{\partial \omega} = 0, \quad \frac{\partial \tau}{\partial n} = 0, \quad \frac{\partial^2 \tau}{\partial \omega^2} < 0, \quad \frac{\partial^4 \tau}{\partial \omega^2 \partial n^2} - \left( \frac{\partial^2 \tau}{\partial \omega \partial n} \right)^2 > 0 \quad (12)$$

Then the corresponding characteristic wavelengths in the axial and circumferential directions are designated as  $2\pi/\omega_f$  and  $2\pi R/n_f$ , respectively.

#### 4 Examples and discussions

For conciseness, introduce the following dimensionless parameters

$$\bar{\tau} = 3\mu\tau/\gamma, \quad \bar{\omega} = \omega R, \quad \bar{\lambda} = 2\pi/\bar{\omega}, \quad \chi = \rho^2 R/(2\epsilon\gamma) \quad (13)$$

Fig.3 shows the dimensionless growth rate  $\bar{\tau}$  as a function of the normalized wavenumber  $\bar{\omega}$  along the axial direction and the mode-number  $n$  along the circumferential direction, where  $\chi = 0.5$ . It is seen that the critical plane  $\bar{\tau} = 0$  corresponds to a curve of critical modes  $(n_c, \bar{\omega}_c)$ , at which the growth rate is zero. The surface of the soft fiber is unstable in the range of  $\bar{\omega} \in (0, \bar{\omega}_c)$  and  $n \in (0, n_c)$ , i.e., above the critical plane  $\bar{\tau} = 0$ . The electric field serves as the main driving force of instability. Due to the perturbation, the electrostatic pressure on the film surface will become nonuniform and its gradient drives the viscous fluid flow from the troughs to the crests and increases the amplitude of the perturbation. Noticeably, the fastest growth rate usually occurs at  $n = 0$ , as also illustrated in Fig. 4. In other words, the cylindrical fiber tends to be destabilized with an axi-symmetrical mode. In the sequel, we will mainly address this special case.

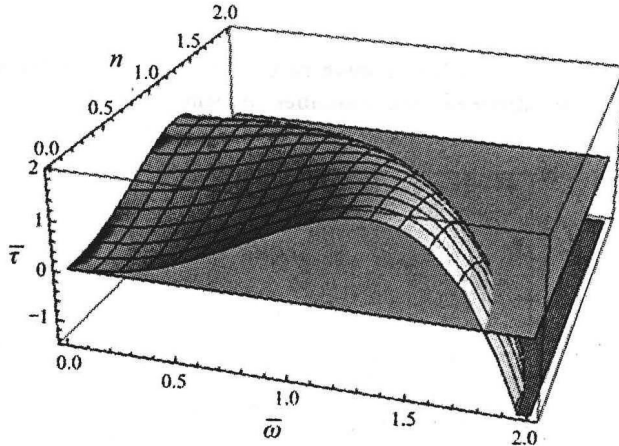


Fig. 3 The dependence of the growth rate  $\bar{\tau}$  on the wavenumber  $\bar{\omega}$  and the mode-number  $n$ , where  $\chi = 0.5$

The effects of charge density and fiber radius on the axi-symmetrical instability characteristic of the fiber surface are plotted in Fig.5 and Fig.6. It is found that the larger the surface charge density, the bigger the growth rate. Both the critical wavenumber and the most probable



wavenumber increase with the increase in the fiber radius  $R$  and the surface charge density  $\rho^2$ . Inversely, the normalized wavelengths  $\bar{\lambda}_r$  and  $\bar{\lambda}_c$  decrease with the increases in  $\rho^2$  and  $R$  but increase with increasing  $\gamma$ . When  $\chi = 0$ , i.e., the surface charges vanish, the fiber surface also behaves as a Rayleigh-like instability due to surface tension. This indicates that, on a cylindrical surface, the surface tension plays a destabilizing role in the surface evolution, which is different from the planar or even spherical surface. Furthermore, the Rayleigh-like instability<sup>[14]</sup> takes on a relative long wavelength ( $2\sqrt{2}\pi R$ ), while the surface charges suppress the wavelength. In addition, the present model predicts that positive and negative surface charges act as the same role in destabilizing the fiber surface.

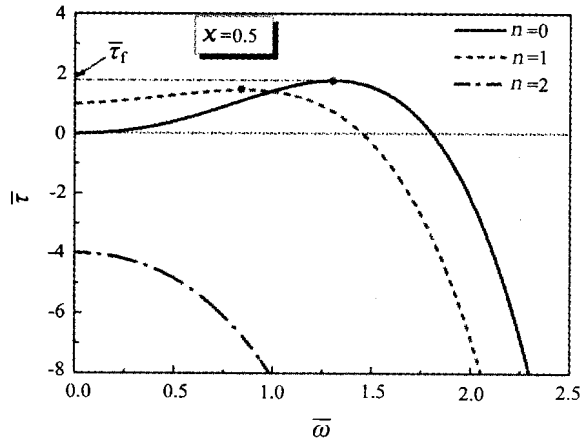


Fig. 4 The variation of the growth rate  $\bar{\tau}$  versus the wavenumber  $\bar{\omega}$  for different mode-number  $n$ , where  $\chi = 0.5$

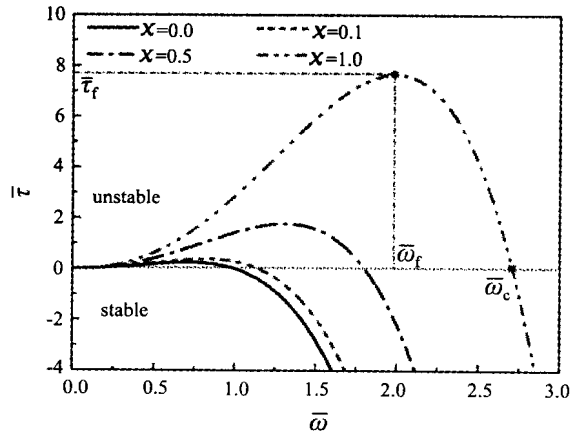


Fig. 5 The variation of the growth rate  $\bar{\tau}$  versus the wavenumber  $\bar{\omega}$  for different  $\chi$ , where  $n = 0$